Report

Cell Reports

# Network-Targeted, Multi-site Direct Cortical Stimulation Enhances Working Memory by Modulating Phase Lag of Low-Frequency Oscillations

## Graphical Abstract

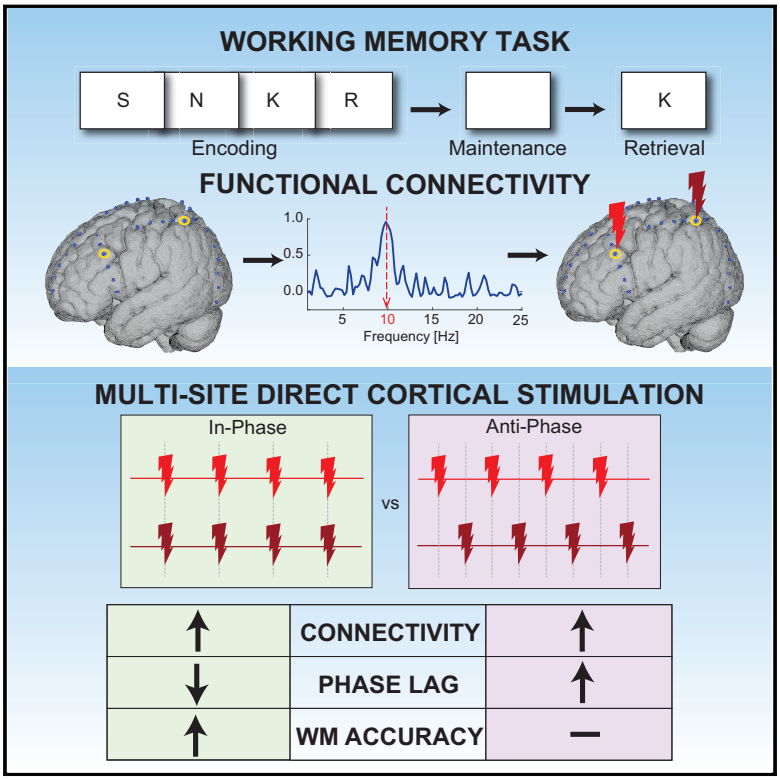


## Highlights

- Multiple nodes of working memory network are targeted using direct cortical stimulation
- In-phase stimulation increases performance relative to sham stimulation
- In-phase and anti-phase stimulation modulates phase lag in opposite directions

## Authors

Sankaraleengam Alagapan, Justin Riddle, Wei Angel Huang, Eldad Hadar, Hae Won Shin, Flavio Fröhlich

## Correspondence

flavio_frohlich@med.unc.edu

## In Brief

Alagapan et al. use intracranial stimulation to simultaneously target multiple nodes of the working memory network. Functional connectivity within the network increases with stimulation, while task performance and phase lag between nodes in the network depend on the relative timing between stimulation.

Alagapan et al., 2019, Cell Reports *29*, 2590–2598
November 26, 2019 
https://doi.org/10.1016/j.celrep.2019.10.072

CellPress

OPEN ACCESS
CellPress

Cell Reports
Report

# Network-Targeted, Multi-site Direct Cortical Stimulation Enhances Working Memory by Modulating Phase Lag of Low-Frequency Oscillations

Sankaraleengam Alagapan,[1,2] Justin Riddle,[1,2] Wei Angel Huang,[2] Eldad Hadar,[3] Hae Won Shin,[3,4] and Flavio Fröhlich[1,2,4,5,6,7,8,*]

[1]Carolina Center for Neurostimulation, University of North Carolina at Chapel Hill, Chapel Hill, NC 27599, USA
[2]Department of Psychiatry, University of North Carolina at Chapel Hill, Chapel Hill, NC 27599, USA
[3]Department of Neurosurgery, University of North Carolina at Chapel Hill, Chapel Hill, NC 27599, USA
[4]Department of Neurology, University of North Carolina at Chapel Hill, Chapel Hill, NC 27599, USA
[5]Department of Cell Biology and Physiology, University of North Carolina at Chapel Hill, Chapel Hill, NC 27599, USA
[6]Department of Biomedical Engineering, University of North Carolina at Chapel Hill, Chapel Hill, NC 27599, USA
[7]Neuroscience Center, University of North Carolina at Chapel Hill, Chapel Hill, NC 27599, USA
[8]Lead Contact
*Correspondence: flavio_frohlich@med.unc.edu
https://doi.org/10.1016/j.celrep.2019.10.072

## SUMMARY

**Working memory is mediated by the coordinated activation of frontal and parietal cortices occurring in the theta and alpha frequency ranges. Here, we test whether electrically stimulating frontal and parietal regions at the frequency of interaction is effective in modulating working memory. We identify working memory nodes that are functionally connected in theta and alpha frequency bands and intracranially stimulate both nodes simultaneously in participants performing working memory tasks. We find that in-phase stimulation results in improvements in performance compared to sham stimulation. In addition, in-phase stimulation results in decreased phase lag between regions within working memory network, while anti-phase stimulation results in increased phase lag, suggesting that shorter phase lag in oscillatory connectivity may lead to better performance. The results support the idea that phase lag may play a key role in information transmission across brain regions. Thus, brain stimulation strategies to improve cognition may require targeting multiple nodes of brain networks.**

## INTRODUCTION

Working memory (WM) is an important component of cognition and supports higher cognitive functions in humans such as fluid intelligence, decision making, and learning. The impairment of WM is observed in many psychiatric and neurological disorders (Allen et al., 2010; Baddeley et al., 1991; Lee and Park, 2005) and is often not addressed by contemporary treatment strategies. Thus, approaches that can improve WM are required. The neural substrates of WM are spread across frontal, cingulate, and parietal cortices (Nee et al., 2013; Owen et al., 2005; Rottschy et al., 2012; Wager and Smith, 2003) and are thought to be coordinated by cortical oscillations. Theta (4–8 Hz) and alpha (8–12 Hz) oscillations are known to play a critical role in WM (Gevins et al., 1997; Jensen et al., 2002; Jensen and Tesche, 2002; Raghavachari et al., 2001). Results from neuroimaging studies suggest that fronto-parietal connectivity may play an important role in WM (Dima et al., 2014; Harding et al., 2015; Ma et al., 2012). Electroencephalography (EEG) and magnetoencephalography (MEG) studies have shown that fronto-parietal connectivity may be characterized by interactions in different oscillatory frequency bands. Alpha band phase synchronization in fronto-parietal regions has been shown to be modulated by WM load (Palva et al., 2010; Zanto et al., 2011). Theta band connectivity has been shown to increase with increased central executive demands (Payne and Kounios, 2009; Sauseng et al., 2005b). The neural substrate for WM is a network of brain regions, and thus any strategy that targets WM may be better served by engaging multiple nodes of the network.

Noninvasive brain stimulation methods such as rhythmic transcranial magnetic stimulation (rTMS), in which a periodic pulse train is applied, and transcranial alternating current stimulation (tACS), in which a continuous sinusoidal alternating current is applied, allow for targeting neural oscillations by matching the stimulation frequency to the frequency of oscillations (Fröhlich, 2015). Most of these studies (Albouy et al., 2017; Alekseichuk et al., 2016; Esslinger et al., 2014; Hoy et al., 2016; Jaušovec et al., 2014) have focused on stimulating a single region. In contrast, studies in which multiple regions of the WM network are targeted have yielded important insights into functional network properties. tACS studies have shown that stimulating fronto-parietal networks using waveforms that have 0° phase offset (in-phase stimulation) results in the improvement of WM performance, while stimulating networks using waveforms that have 180° phase offset (anti-phase stimulation) results in the deterioration of performance (Polanía et al., 2012; Violante et al., 2017). In-phase stimulation was hypothesized to cause synchronization of the fronto-parietal networks, while anti-phase stimulation was hypothesized to cause de-synchronization.

 

Neuroimaging during stimulation indicated increased blood oxygenation level-dependent (BOLD) signals in WM regions during in-phase stimulation, while functional connectivity increased with both in-phase stimulation and anti-phase stimulation (Violante et al., 2017). The BOLD signal does not have millisecond temporal resolution and thus precluded any analysis of the changes in oscillatory network activity.

Compared to transcranial electric stimulation, direct cortical stimulation (DCS), in which electrical stimulation is applied directly on the cortical surface, offers higher spatial specificity. In addition, intracranial EEG (iEEG) provides higher spatial resolution relative to EEG or MEG and higher temporal resolution relative to functional neuroimaging. Thus, by combining DCS and iEEG, it is possible to dissect functional networks with high spatiotemporal precision. This approach has been used for causally perturbing the electrophysiological and anatomical substrates of episodic memory (Ezzyat et al., 2018; Kucewicz et al., 2018; Suthana et al., 2012). DCS has also been used to target networks engaged in spatial memory (Siegle and Wilson, 2014), but stimulation resulted in the impairment of performance (Kim et al., 2018). In another study, the direct stimulation of bilateral hippocampal regions with in-phase and anti-phase stimulation resulted in trend-level changes in performance (Fell et al., 2013). Using this approach, we have shown that frequency-matched DCS of a region (left superior frontal gyrus) that exhibited low-frequency oscillatory activity results in WM improvement (Alagapan et al., 2019a). Here, we extended our stimulation protocol to target networks underlying WM by stimulating two functionally connected regions simultaneously. We used a measure of phase synchronization, the weighted phase lag index, to identify regions that are functionally connected in alpha and theta frequency bands during a Sternberg WM task. We applied periodic pulse stimulation in-phase and anti-phase, matched to the frequency of functional interactions, to the two functionally connected regions and compared the performance against sham stimulation. We hypothesized that in-phase stimulation would result in an increase in oscillatory functional connectivity relative to sham and thereby improve WM performance, while anti-phase stimulation would result in a decrease in oscillatory functional connectivity relative to sham and thereby impair WM performance. While in-phase stimulation improved performance, anti-phase stimulation did not impair performance relative to sham. Analysis of functional connectivity properties in the meta-analysis-based WM (mWM) network revealed that functional connectivity was increased by both in-phase and anti-phase stimulation. However, in-phase stimulation decreased phase lag relative to sham between regions within the mWM network, while anti-phase stimulation increased phase lag relative to sham, suggesting a non-linear relation between the phase lag of connections within a network and performance.

## RESULTS

We performed network-targeted stimulation in all of the participants implanted with subdural strips and stereo-EEG electrodes when performing a Sternberg WM task (Figure 1). In the baseline session, the WM load, defined as the number of items to be held in WM, was varied pseudo-randomly for each trial. The WM load for each participant was titrated according to performance in a short practice session (3, 5 for P1; 5, 7 for P2 and P3). The chi-square test did not reveal any significant influence of list length on accuracy ($\chi^2 = 0.434$, df = 2, p = 0.805). Analysis of reaction time did not reveal any significant influence of list length (linear mixed effects model with list length as the fixed factor and participant as the random factor; $F_{2,175.51} = 0.630$, p = 0.534). The reaction time and accuracy for individual participants are shown in Figure S2.

Analysis of functional connectivity using debiased weighted phase lag index (dWPLI) revealed oscillatory interactions in theta and alpha frequency bands. dWPLI measures the degree of consistency of phase lag between two signals and is not affected by volume conduction (Vinck et al., 2011), making it an effective tool for identifying functional interactions in iEEG. In P1, electrodes that exhibited connectivity within the left frontal regions (superior frontal gyrus and inferior precentral gyrus) in the theta band (4 Hz) were chosen. In P2, electrodes in the left frontal and parietal regions (inferior frontal junction and superior parietal lobule) that exhibited interactions in the alpha band (9 Hz) interactions were chosen. In P3, no strong functional interactions were observed (apart from the interactions between neighboring electrodes). Therefore, we chose electrodes that were in the putative WM network in the right hemisphere (middle frontal gyrus and superior intraparietal sulcus). We chose 10 Hz as the stimulation frequency for P3, as alpha band synchronization between frontal and parietal regions has been shown to affect WM (Palva et al., 2010; Zanto et al., 2011). The mean dWPLIs for the electrodes chosen are shown in Figure 2A. Post hoc analysis of the spatial proximity of the chosen stimulation electrodes to the canonical WM network identified from an automated meta-analysis (Yarkoni et al., 2011) revealed that both of the electrode pairs in P2 and P3 were in or near regions that are active during WM (Figure 2B). In P1, one electrode pair was near the inferior frontal junction, another prominent WM region (Nee et al., 2013), and one pair was on the superior frontal gyrus, a region that we have previously demonstrated to be involved in WM.

In the stimulation session, participants performed the Sternberg task again, but with only one level of WM load. Stimulation was applied between pairs of electrodes identified in the baseline session during the encoding epoch. In-phase stimulation resulted in increased accuracy relative to sham in all three participants (Figure 3, top). The chi-square test with all three conditions revealed a statistically significant association between condition and trial accuracy ($\chi^2 = 7.315$, df = 2, p = 0.026). Further pairwise comparisons revealed that in-phase stimulation increased accuracy relative to sham ($\chi^2 = 6.429$, df = 1, p = 0.011), but there was no difference in accuracy for anti-phase relative to sham ($\chi^2 = 1.0913$, df = 1, p = 0.296) or in-phase relative to anti-phase ($\chi^2 = 1.847$, df = 1, p = 0.174). Thus, network-targeted stimulation improved WM accuracy, but only when both electrode pairs were stimulated simultaneously without phase lag. The analysis of reaction time did not reveal any statistically significant effect of stimulation condition (Figure 3, bottom, linear mixed model with fixed factor stimulation condition and random factor participant; $F_{2,223.42} = 0.545$, p = 0.581).

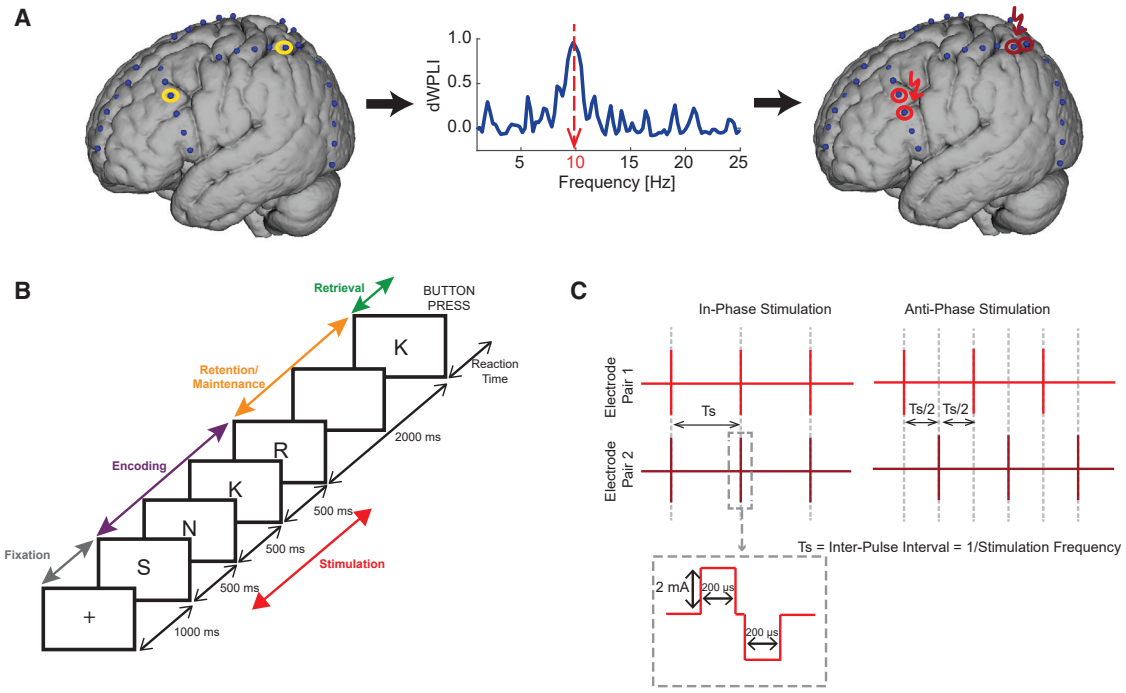


**Figure 1. Schematic of Network-Targeted Stimulation**

(A) Intracranial EEG data from implanted electrodes, collected when participants performed WM tasks, are processed to identify functionally connected regions that are then targeted with direct cortical stimulation.

(B) Sternberg WM task depicting the different epochs and timing of the components of each epoch.

(C) The stimulation paradigms used in the study. Each vertical red line denotes a biphasic pulse. In-phase stimulation consists of pulses applied simultaneously to functionally connected regions without any phase offset (time delay). Anti-phase stimulation consists of pulses applied with a phase offset of 180° (time delay of half the inter-stimulus interval Ts). Dotted lines are provided for visual guidance.

DCS introduces electrical stimulation artifacts in iEEG that must be addressed before analyses can be performed. We used an independent component analysis (ICA)-based method to remove the stimulation artifacts. Following artifact removal, we computed dWPLI between electrodes that were in the mWM network. As an exploratory measure, we computed magnitude-squared coherence, which is used widely in connectivity analyses of oscillatory networks. Coherence provides a complementary measure of functional connectivity, as it accounts for the correlations in spectral power, which is not captured by dWPLI. We restricted our analysis to the bands around the stimulation frequency for each individual participant. In addition, we used a permutation-based approach as described in Method Details (Estimation of Functional Connectivity) to identify those network connections that exhibited statistically significant pairwise differences between the conditions (in-phase stimulation versus sham stimulation, anti-phase stimulation versus sham stimulation, and in-phase stimulation versus anti-phase stimulation). This resulted in a network with sparse connections between regions within the WM network. Analysis of network sparsity revealed that electrodes outside the WM network had higher edge density (1.982% ± 0.862%, mean ± SEM) compared to electrodes within the WM network (0.411% ± 0.158%, $F_{1,14} = 8.468$, $p = 0.011$, linear mixed effects model with edge density as dependent variable and network as fixed factor and participants as random factor; see Tables S1 and S2 for details on the individual networks after and before false discovery rate [FDR] correction, respectively). We found that in-phase stimulation resulted in increased functional connectivity relative to sham (dWPLI: 0.149 ± 0.015, $F_{1,54} = 4.524$, $p = 0.038$; coherence: 0.142 ± 0.013, $F_{1,63} = 121.46$, $p < 0.001$, linear mixed model). Similarly, anti-phase stimulation resulted in increased functional connectivity relative to sham (dWPLI: 0.156 ± 0.017, $F_{1,45} = 87.434$, $p < 0.001$; coherence: 0.106 ± 0.014, $F_{1,73} = 58.185$, $p < 0.001$). In contrast, there was no significant difference in dWPLI between in-phase and anti-phase stimulation (0.019 ± 0.030, $F_{1,34} = 0.400$, $p = 0.531$), while coherence was higher with in-phase stimulation relative to anti-phase stimulation: 0.085 ± 0.035, $F_{1,14} = 6.201$, $p = 0.026$). We verified the results of the analysis using the one-sample t test (Table S3). The results suggest that contrary to our initial hypothesis, both in-phase and anti-phase stimulation increased functional connectivity relative to sham.

While these results may appear counterintuitive, it should be noted that dWPLI is a measure of phase consistency and does not include any information regarding the actual phase difference. It is conceivable that both in-phase stimulation and anti-phase stimulation successfully engage the network due to the repeated periodic perturbation of the network and increased overall phase consistency. However, since the stimulation differed in phase lag between the targeted electrode pairs, in-phase and anti-phase may have affected the specific phase

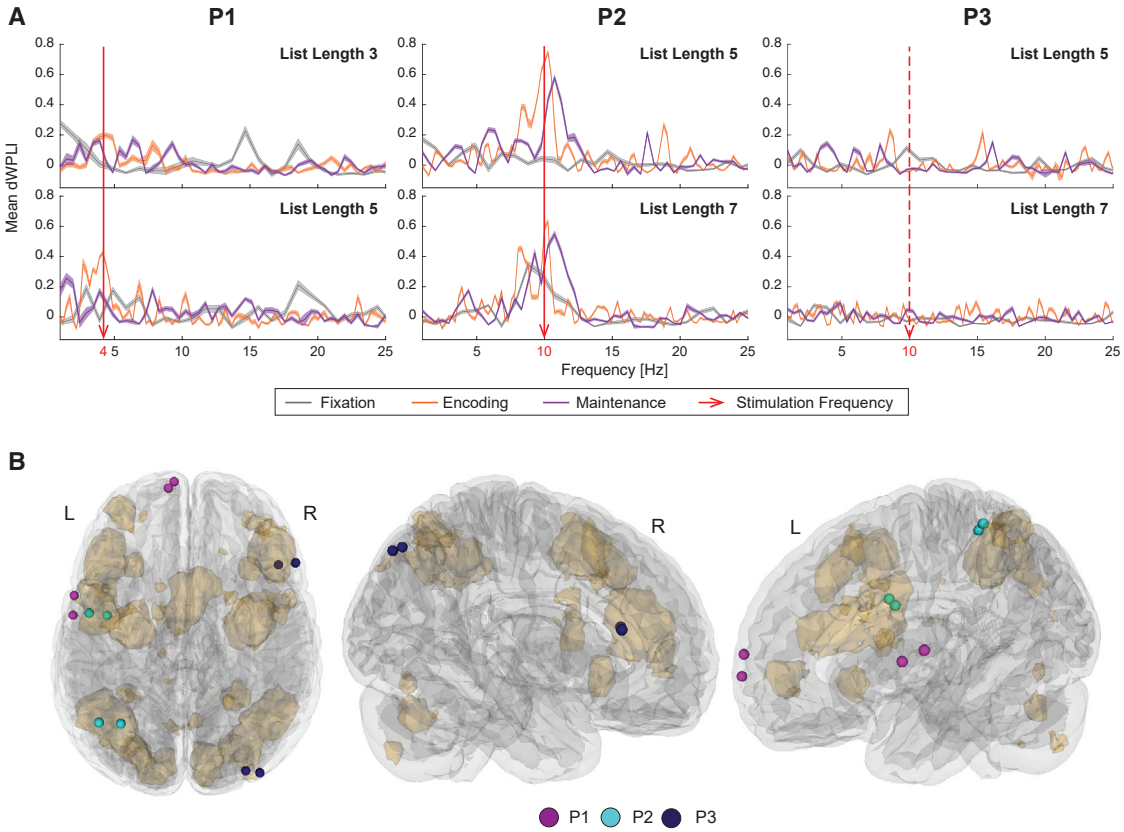


**Figure 2. Functional Connectivity of Stimulation Electrodes**

(A) Mean dWPLI for the stimulation electrodes for the different cognitive loads and the different epochs. Shaded regions denote the jackknife estimate of SD.

(B) The anatomical locations of the identified stimulation electrodes for the three participants. The beige-shaded regions denote WM regions identified from meta-analyses of functional neuroimaging studies.

See also Figure S1.

lag between nodes in the network. To verify this, we computed phase lag at the stimulation frequency between electrode pairs that exhibited significant pairwise dWPLI differences between any of the three stimulation conditions. Phase lag was computed from the cross-spectrum of the iEEG signal during the stimulation epoch. We pooled the data of the three participants together, as the distribution of phase lag for individual participants did not satisfy the assumptions required for the circular statistics. There was a trend-level effect of comparison on the phase lag differences (Figure 4C; Watson-Wheeler test, $W_4$ = 8.058, p = 0.089). We found that in-phase stimulation resulted in an overall decrease in phase lag relative to sham (−0.191 ± 0.823 radians; mean ± SEM), while anti-phase stimulation resulted in an overall increase in phase lag relative to sham (0.221 ± 0.336 radians), indicating that in-phase stimulation and anti-phase stimulation modulate phase lag in opposite directions. In addition, in-phase stimulation decreased phase lag relative to anti-phase stimulation (−0.268 ± 0.239 radians).

## DISCUSSION

In this study, we used a network-targeted stimulation approach to modulate the WM network and thereby improve WM performance. The increased functional connectivity from in-phase stimulation and anti-phase stimulation may have been due to the periodic input of DCS into the WM network that aligned the phase of electrical activity between multiple regions, albeit at different lags. Our results suggest that the differential effect on phase lag may have contributed to the behavioral modulation. Phase synchronization has been hypothesized to enable interareal communication by aligning periods of excitability across regions or by enabling spike timing-dependent plasticity (Fell and Axmacher, 2011; Zanos et al., 2018). Our electrical stimulation occurred at a timescale faster than the typical time frame for observing plasticity, suggesting that our in-phase stimulation may have aligned periods of excitability across regions that enabled enhanced communication. While in-phase stimulation improved performance, we did not observe any impairment in performance with anti-phase stimulation. In fact, anti-phase stimulation also improved performance relative to sham in two of the three participants. This suggests that there may be a general beneficial effect of stimulating functionally connected areas. In-phase stimulation may have reduced communication delay within an optimal window in which information may be effectively transmitted between regions, resulting in improvement in performance. In contrast, anti-phase stimulation may have resulted in

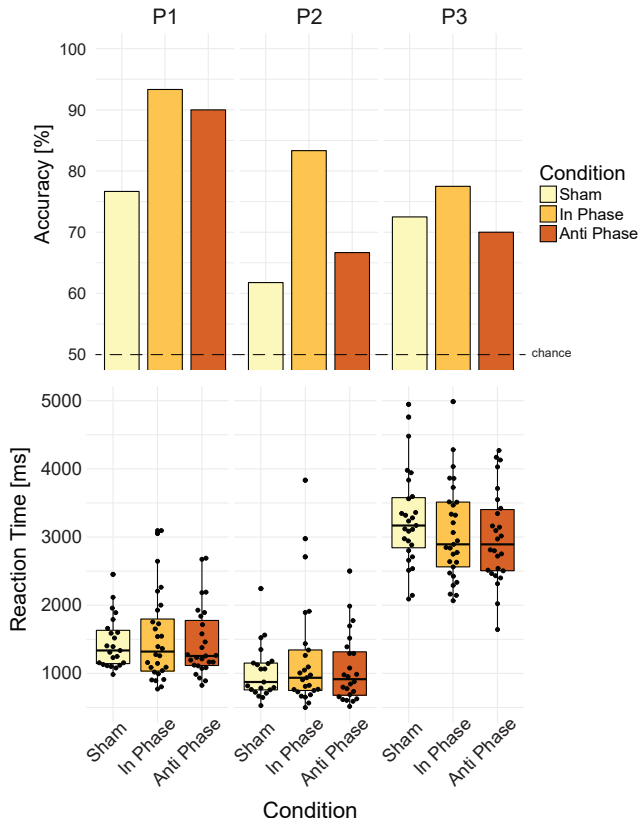


**Figure 3. Effect of Network-Targeted Stimulation on WM Performance**

In-phase stimulation increased accuracy relative to sham (top). Stimulation did not affect reaction time (bottom).

See also Figure S2.

increased communication delays outside this optimal window, which is inconsequential for information transmission and integration. Further studies are required to confirm this specific hypothesis.

Our results follow tACS studies that have shown behavioral effects of stimulation in WM tasks, although we observe improvements in accuracy, while improvements in reaction times are more commonly reported. Polanía et al. (2012) observed a decrease in reaction time with in-phase stimulation and an increase in reaction time with anti-phase stimulation relative to sham. Violante et al. (2017) observed a decrease in reaction time for in-phase stimulation relative to sham and anti-phase stimulation, while there was no difference between sham and anti-phase stimulation, similar to what we observe. In addition, Violante et al. (2017) report increased BOLD signal functional connectivity increases in the WM network for both in-phase and anti-phase stimulation. Although the functional connectivity from BOLD signal quantifies interactions at a slower timescale relative to what is observed in iEEG, these results support our observation that both in-phase and anti-phase stimulation resulted in increased functional connectivity.

We used a hybrid data-driven approach to restrict our analyses to putative WM networks in the three participants. The use of meta-analysis-based priors allowed us to control the dimensionality of our variable of interest, which is the functional interactions between brain regions involved in WM. The WM network we used was derived from a meta-analysis of 1,091 fMRI studies (Yarkoni et al., 2011). However, it must be noted that BOLD activity of regions often corresponds to iEEG activity in high-frequency broadband activity (30–130 Hz) (Ojemann et al., 2013), with lower correlations between lower-frequency band activity. Therefore, it is conceivable that we may have excluded regions that exhibited task-related connectivity. Given the heterogeneity and the small sample size, we made this decision as a necessary trade-off for generalizability at the cost of an exhaustive naive data-driven approach. Nevertheless, we found task-related functional connectivity between regions in or near the mWM network in participants P1 and P2. In P1, we found theta band connectivity between the superior frontal gyrus and the precentral gyrus. Although the superior frontal gyrus is not a part of the mWM network, our previous work has shown it may play a role in WM (Alagapan et al., 2019a). In P2, we found that alpha band connectivity within the mWM network and stimulation resulted in the highest improvement among the three participants. In P3, even with electrodes close to the mWM network, we did not observe any significant functional interaction. This may be due to variability in the functional recruitment of brain regions for this participant. While stimulation resulted in an improvement in WM accuracy, the effect in P3 was weaker than the other two participants, presumably due to the decreased recruitment of these regions by the task. However, the region of cortex activated by intracranial direct cortical stimulation extends farther than the immediate vicinity of the stimulation electrodes on the order of $\sim$50 $mm^3$ (Butson and McIntyre, 2005; Winawer and Parvizi, 2016), while the spatial extent of local field potential (LFP) recordings is a few millimeters (Lempka and McIntyre, 2013). Thus, stimulation may have spread into neighboring regions that are known to be canonically activated by WM task demands.

Oscillations in the theta and alpha frequency bands have been shown to support WM in many studies (Hsieh and Ranganath, 2014; Klimesch, 1999), with increased oscillatory power as a marker for synchronization. Phase synchronization between brain regions in alpha and theta frequency bands have been shown to underlie many memory processes (see reviews by Fell and Axmacher, 2011 and Klimesch et al., 2008), with theta band activity implicated in top-down control (Kawasaki et al., 2010; Polanía et al., 2012; Sauseng et al., 2010) and alpha band activity implicated in the suppression of irrelevant information (Jensen and Mazaheri, 2010; Sauseng et al., 2009). Theta band synchronization has been observed between fronto-temporal and fronto-parietal regions in WM tasks (Axmacher et al., 2008; Daume et al., 2017; Sarnthein et al., 1998; Schack et al., 2005). While fronto-parietal synchronization in the alpha band has been associated with cognitive control and visuospatial attention (Lobier et al., 2018), interareal synchrony has been observed to be modulated by WM load in the retention period (Palva et al., 2010; Sauseng et al., 2005a). Supporting these observations, we found alpha and theta band connectivity in our participants. The variability in the frequency at which interaction was found may be due to differences in strategy (Roux and Uhlhaas, 2014), with theta being dominant in strategies in which sequential information is encoded and alpha being

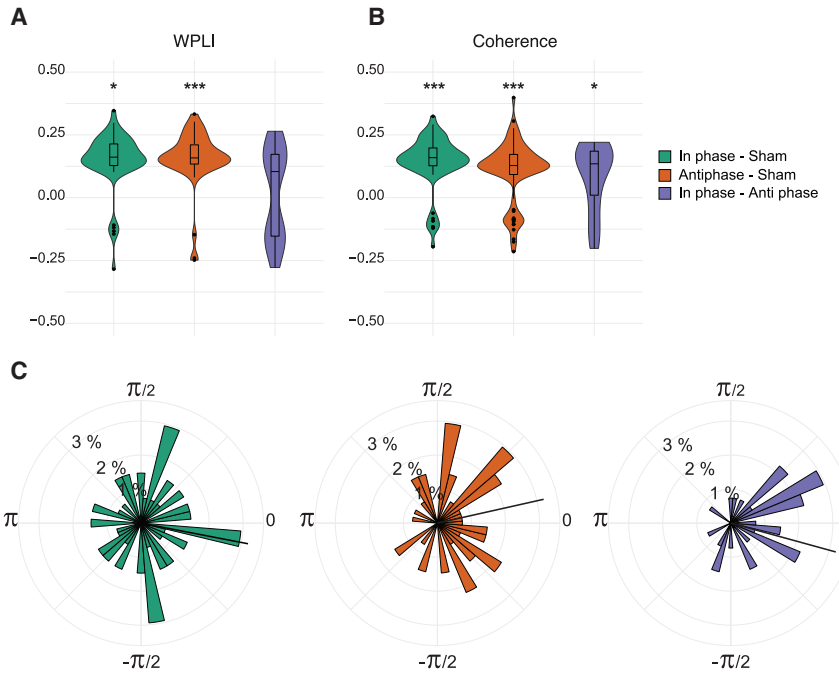


**Figure 4. Effect of Network-Targeted Stimulation on WM Network**

(A) Pairwise difference of dWPLI between stimulation conditions. In-phase versus sham and anti-phase versus sham were significantly greater than 0.

(B) Pairwise difference of coherence between stimulation conditions. All three pairwise differences were significantly greater than 0.

(C) Circular histogram denoting the pairwise differences in phase lag across the three comparisons for the three participants. The black line denotes the mean phase lag difference for each comparison.

*$p < 0.05$ in a linear mixed model; ***$p < 0.001$.

See also Tables S1, S2, and S3.

dominant in strategies in which competing information is suppressed. Alternately, the differences could be driven by the difference in regions between which functional connectivity is observed. We observed theta between electrodes within frontal regions, while alpha was observed between electrodes in frontal and parietal regions. The studies mentioned above are constrained by the limitations of EEG, which has poor spatial resolution and is highly susceptible to volume conduction. The use of iEEG, which has higher spatial resolution relative to EEG (millimeters versus centimeters) and dWPLI, which by design is not affected by volume conduction, enabled us to overcome these limitations and provide a more fine-grained picture of the functional interactions. The use of bipolar stimulation montage allowed us to constrain the area of stimulation. While bipolar referencing for the recorded data would allow us to localize the sources of oscillatory activity, the referencing may distort phases, with distortion possibly contributed by electrodes outside the WM network. This is an inherent limitation of iEEG, in which the spacing between electrodes may be larger than individual sources of oscillatory activity.

While these results provide important insight into the role phase lag may play in coordinating WM, the heterogeneity and the small sample size limits the interpretation to a general population. The limited sample size and inconsistency of electrode locations precluded us from performing a standardization of connectivity across subjects at a gyri/sulci level. In addition, standardizing based on lobe confounds multiple networks that are known to be anti-correlated or serve different cognitive functions (e.g., the default mode network and the task-positive network both have prominent nodes in the frontal and parietal lobes). Therefore, we pooled connections across participants using an *a priori* network that should be activated during the Sternberg task and do not make any inference about the anatomical specificity of our stimulation effects.

In addition, the phase lag between stimulation sites was not taken into consideration, as the initial hypothesis was based on the consistency of phase synchronization. In contrast to our approach, Kim et al. (2018) stimulated hubs of a memory-retrieval network at the phase lag observed between the two nodes, but they found that stimulation impaired performance. Our results imply that choosing a phase lag that is shorter than the observed phase lag may be beneficial. The choice of stimulation parameters was limited to in-phase stimulation and anti-phase stimulation to ensure enough trials in each condition for statistical analysis. However, this meant that we were not able to directly confirm whether the effect is frequency specific. Further studies incorporating arrhythmic stimulation as used in some TMS studies can be used to establish the frequency specificity of stimulation effects (Albouy et al., 2017; Quentin et al., 2016). It must also be noted that the use of dWPLI precludes us from testing the importance of zero-lag communication, which has been shown to be important for neuronal communication (Fries, 2015). Periodic stimulation using noninvasive and invasive approaches has been shown to improve cognitive performance (Albouy et al., 2017; Hanslmayr et al., 2019; Luber et al., 2007; Suthana et al., 2012), while disruption has also been demonstrated (Gagnon et al., 2010; Mottaghy, 2006; Osaka et al., 2007; Postle et al., 2006; Riddle et al., 2019). Periodic stimulation at low current levels could serve to align neural oscillators, thereby increasing communication efficacy (Hanslmayr et al., 2019; Thut et al., 2011). Our results support this hypothesis, suggesting that periodic stimulation may help the entrainment of oscillations.

We did not observe an effect of WM load on reaction time or accuracy in the baseline session. Reaction time follows a monotonic increase with increasing WM load when participants are required to remember the order of items presented (Corbin and Marquer, 2013). Since we did not require our participants to remember the order of items, participants may have used alternate strategies to perform the task (Corbin and Marquer, 2009). However, as we set the WM load constant in the stimulation session, we are able to control for these potential differences in strategy for the primary analysis that is run on differences in performance based on inter-leaved stimulation conditions.

We used an ICA-based approach for removing stimulation artifacts. ICA is effective in removing stimulation artifacts such that signals at the stimulation frequency can be recovered with high reliability, as we have demonstrated previously (Alagapan et al., 2019a, 2019b). However, artifacts at higher harmonics are typically hard to eliminate using ICA and may require other approaches. Therefore, we restricted our analysis to the stimulation frequency. In addition, stimulation artifacts, if present, would have led to increased functional connectivity at zero phase lag due to volume conduction. Since dWPLI does not incorporate zero phase lag connectivity, the observed increases in dWPLI are less likely to have resulted from stimulation artifacts.

While many studies quantify phase synchronization as consistency in phase differences, very few studies have focused on the phase lag between regions (Polanía et al., 2012). Given the recent findings on phase-dependent information processing (Kerren et al., 2018; Zoefel et al., 2018), our result highlights the importance of considering phase information when studying functional interactions between brain regions. Overall, these findings advance our understanding of network-targeted stimulation for improving cognition in humans. Our results provide causal evidence that networks of brain regions are critical to cognition (Bassett and Sporns, 2017; Kopell et al., 2014) and that optimal stimulation may require multi-site stimulation. This work may ultimately lead to therapeutic benefits for cognitive deficits that accompany many neurological and psychiatric disorders.

## STAR★METHODS

Detailed methods are provided in the online version of this paper and include the following:

- KEY RESOURCES TABLE
- LEAD CONTACT AND MATERIALS AVAILABILITY
- EXPERIMENTAL MODEL AND SUBJECT DETAILS
  - Participants
- METHOD DETAILS
  - Working Memory Task
  - ECoG Data Acquisition and Direct Cortical Stimulation
  - Removal of Electrical Stimulation Artifacts
  - Identification of Electrode Locations
  - Determining Meta-Analysis-Based WM Network
- QUANTIFICATION AND STATISTICAL ANALYSIS
  - Data Analysis
  - Selection of Stimulation Electrodes
  - Estimation of Functional Connectivity
  - Statistical Analysis
- DATA AND CODE AVAILABILITY

## SUPPLEMENTAL INFORMATION

Supplemental Information can be found online at https://doi.org/10.1016/j.celrep.2019.10.072.

## ACKNOWLEDGMENTS

The authors thank the members of the Frohlich lab for their valuable input. The authors also thank the EEG technicians at the NC Neurosciences Hospital Epilepsy Monitoring Unit for their generous help with the iEEG recordings. The research reported in this publication was supported in part by the National Institute of Mental Health under award numbers R01MH101547 and R21MH105557 and the National Institute of Neurological Disorders and Stroke under award number R21NS094988-01A1. The content is solely the responsibility of the authors and does not necessarily represent the official views of the National Institutes of Health (NIH).

## AUTHOR CONTRIBUTIONS

S.A., H.W.S., and F.F. designed the experiments; S.A., J.R., W.A.H., E.H., and H.W.S. performed the electrophysiological recordings; S.A. and J.R. analyzed the data; and S.A., J.R., W.A.H., E.H., H.W.S., and F.F. prepared the manuscript.

## DECLARATION OF INTERESTS

F.F. is the lead inventor of intellectual property filed on the topics of noninvasive brain stimulation by UNC. F.F. is the founder, chief scientific officer (CSO), and majority owner of Pulvinar Neuro LLC, which played no role in this research. The other authors declare no competing interests.

Received: January 18, 2019
Revised: June 10, 2019
Accepted: October 17, 2019
Published: November 26, 2019

## REFERENCES

Accolla, E.A., HerrojoRuiz, M., Horn, A., Schneider, G.H., Schmitz-Hübsch, T., Draganski, B., and Kühn, A.A. (2016). Brain networks modulated by subthalamic nucleus deep brain stimulation. Brain *139*, 2503–2515.

Alagapan, S., Schmidt, S.L., Lefebvre, J., Hadar, E., Shin, H.W., and Fröhlich, F. (2016). Modulation of Cortical Oscillations by Low-Frequency Direct Cortical Stimulation Is State-Dependent. PLoS Biol. *14*, e1002424.

Alagapan, S., Lustenberger, C., Hadar, E., Shin, H.W., and Fröhlich, F. (2019a). Low-frequency direct cortical stimulation of left superior frontal gyrus enhances working memory performance. Neuroimage *184*, 697–706.

Alagapan, S., Shin, H.W., Fröhlich, F., and Wu, H.T. (2019b). Diffusion geometry approach to efficiently remove electrical stimulation artifacts in intracranial electroencephalography. J. Neural Eng. *16*, 036010.

Albouy, P., Weiss, A., Baillet, S., and Zatorre, R.J. (2017). Selective Entrainment of Theta Oscillations in the Dorsal Stream Causally Enhances Auditory Working Memory Performance. Neuron *94*, 193–206.e5.

Alekseichuk, I., Turi, Z., Amador de Lara, G., Antal, A., and Paulus, W. (2016). Spatial Working Memory in Humans Depends on Theta and High Gamma Synchronization in the Prefrontal Cortex. Curr. Biol. *26*, 1513–1521.

Allen, D.N., Randall, C., Bello, D., Armstrong, C., Frantom, L., Cross, C., and Kinney, J. (2010). Are working memory deficits in bipolar disorder markers for psychosis? Neuropsychology *24*, 244–254.

Axmacher, N., Schmitz, D.P., Wagner, T., Elger, C.E., and Fell, J. (2008). Interactions between medial temporal lobe, prefrontal cortex, and inferior temporal regions during visual working memory: a combined intracranial EEG and functional magnetic resonance imaging study. J. Neurosci. *28*, 7304–7312.

Baddeley, A.D., Bressi, S., Della Sala, S., Logie, R., and Spinnler, H. (1991). The decline of working memory in Alzheimer's disease. A longitudinal study. Brain *114*, 2521–2542.

Bassett, D.S., and Sporns, O. (2017). Network neuroscience. Nat. Neurosci. *20*, 353–364.

Bassett, D.S., Wymbs, N.F., Porter, M.A., Mucha, P.J., Carlson, J.M., and Grafton, S.T. (2011). Dynamic reconfiguration of human brain networks during learning. Proceedings of the National Academy of Sciences *108*, 7641–7646.

Benjamini, Y., and Hochberg, Y. (1995). Controlling the false discovery rate: a practical and powerful approach to multiple testing. J. R. Statist. Soc. *57*, 289–300.

Bennett, C.M., Wolford, G.L., and Miller, M.B. (2009). The principled control of false positives in neuroimaging. Soc. Cogn. Affect. Neurosci. *4*, 417–422.

Brainard, D.H. (1997). The Psychophysics Toolbox. Spat. Vis. *10*, 433–436.

Brett, M., Anton, J.L., Valabregue, R., and Poline, J.-B. (2002). Region of interest analysis using an SPM toolbox. Presented at the 8th International Conference on Functional Mapping of the Human Brain, June 2-6, 2002, Sendai, Japan. Neuroimage *13*, 210–217.

Butson, C.R., and McIntyre, C.C. (2005). Tissue and electrode capacitance reduce neural activation volumes during deep brain stimulation. Clin. Neurophysiol. *116*, 2490–2500.

Corbin, L., and Marquer, J. (2009). Individual differences in Sternberg's memory scanning task. Acta Psychol. (Amst.) *131*, 153–162.

Corbin, L., and Marquer, J. (2013). Is Sternberg's Memory Scanning Task Really a Short-Term Memory Task? Swiss J. Psychol. *72*, 181–196.

Daume, J., Gruber, T., Engel, A.K., and Friese, U. (2017). Phase-Amplitude Coupling and Long-Range Phase Synchronization Reveal Frontotemporal Interactions during Visual Working Memory. J. Neurosci. *37*, 313–322.

Delorme, A., and Makeig, S. (2004). EEGLAB: an open source toolbox for analysis of single-trial EEG dynamics including independent component analysis. J. Neurosci. Methods *134*, 9–21.

Dima, D., Jogia, J., and Frangou, S. (2014). Dynamic causal modeling of load-dependent modulation of effective connectivity within the verbal working memory network. Hum. Brain Mapp. *35*, 3025–3035.

Esslinger, C., Schüler, N., Sauer, C., Gass, D., Mier, D., Braun, U., Ochs, E., Schulze, T.G., Rietschel, M., Kirsch, P., and Meyer-Lindenberg, A. (2014). Induction and quantification of prefrontal cortical network plasticity using 5 Hz rTMS and fMRI. Hum. Brain Mapp. *35*, 140–151.

Ezzyat, Y., Wanda, P.A., Levy, D.F., Kadel, A., Aka, A., Pedisich, I., Sperling, M.R., Sharan, A.D., Lega, B.C., Burks, A., et al. (2018). Closed-loop stimulation of temporal cortex rescues functional networks and improves memory. Nat. Commun. *9*, 365.

Fedorov, A., Beichel, R., Kalpathy-Cramer, J., Finet, J., Fillion-Robin, J.C., Pujol, S., Bauer, C., Jennings, D., Fennessy, F., Sonka, M., et al. (2012). 3D Slicer as an image computing platform for the Quantitative Imaging Network. Magn. Reson. Imaging *30*, 1323–1341.

Fell, J., and Axmacher, N. (2011). The role of phase synchronization in memory processes. Nat. Rev. Neurosci. *12*, 105–118.

Fell, J., Staresina, B.P., Do Lam, A.T., Widman, G., Helmstaedter, C., Elger, C.E., and Axmacher, N. (2013). Memory modulation by weak synchronous deep brain stimulation: a pilot study. Brain Stimul. *6*, 270–273.

Fonov, V., Evans, A.C., Botteron, K., Almli, C.R., McKinstry, R.C., and Collins, D.L.; Brain Development Cooperative Group (2011). Unbiased average age-appropriate atlases for pediatric studies. Neuroimage *54*, 313–327.

Fries, P. (2015). Rhythms for Cognition: Communication through Coherence. Neuron *88*, 220–235.

Fröhlich, F. (2015). Experiments and models of cortical oscillations as a target for noninvasive brain stimulation. Prog. Brain Res. *222*, 41–73.

Gagnon, G., Blanchet, S., Grondin, S., and Schneider, C. (2010). Paired-pulse transcranial magnetic stimulation over the dorsolateral prefrontal cortex interferes with episodic encoding and retrieval for both verbal and non-verbal materials. Brain Res. *1344*, 148–158.

Genovese, C.R., Lazar, N.A., and Nichols, T. (2002). Thresholding of statistical maps in functional neuroimaging using the false discovery rate. Neuroimage *15*, 870–878.

Gevins, A., Smith, M.E., McEvoy, L., and Yu, D. (1997). High-resolution EEG mapping of cortical activation related to working memory: effects of task difficulty, type of processing, and practice. Cereb. Cortex *7*, 374–385.

Hanslmayr, S., Axmacher, N., and Inman, C.S. (2019). Modulating Human Memory via Entrainment of Brain Oscillations. Trends Neurosci. *42*, 485–499.

Harding, I.H., Yücel, M., Harrison, B.J., Pantelis, C., and Breakspear, M. (2015). Effective connectivity within the frontoparietal control network differentiates cognitive control and working memory. Neuroimage *106*, 144–153.

Hoy, K.E., Bailey, N., Michael, M., Fitzgibbon, B., Rogasch, N.C., Saeki, T., and Fitzgerald, P.B. (2016). Enhancement of Working Memory and Task-Related Oscillatory Activity Following Intermittent Theta Burst Stimulation in Healthy Controls. Cereb. Cortex *26*, 4563–4573.

Hsieh, L.T., and Ranganath, C. (2014). Frontal midline theta oscillations during working memory maintenance and episodic encoding and retrieval. Neuroimage *85*, 721–729.

Jaušovec, N., Jaušovec, K., and Pahor, A. (2014). The influence of theta transcranial alternating current stimulation (tACS) on working memory storage and processing functions. Acta Psychol. (Amst.) *146*, 1–6.

Jensen, O., and Mazaheri, A. (2010). Shaping functional architecture by oscillatory alpha activity: gating by inhibition. Front. Hum. Neurosci. *4*, 186.

Jensen, O., and Tesche, C.D. (2002). Frontal theta activity in humans increases with memory load in a working memory task. Eur. J. Neurosci. *15*, 1395–1399.

Jensen, O., Gelfand, J., Kounios, J., and Lisman, J.E. (2002). Oscillations in the alpha band (9-12 Hz) increase with memory load during retention in a short-term memory task. Cereb. Cortex *12*, 877–882.

Kawasaki, M., Kitajo, K., and Yamaguchi, Y. (2010). Dynamic links between theta executive functions and alpha storage buffers in auditory and visual working memory. Eur. J. Neurosci. *31*, 1683–1689.

Kerren, C., Linde-Domingo, J., Hanslmayr, S., and Wimber, M. (2018). An Optimal Oscillatory Phase for Pattern Reactivation during Memory Retrieval. Curr. Biol. *28*, 3383–3392.e6.

Kim, K., Schedlbauer, A., Rollo, M., Karunakaran, S., Ekstrom, A.D., and Tandon, N. (2018). Network-based brain stimulation selectively impairs spatial retrieval. Brain Stimul. *11*, 213–221.

Klimesch, W. (1999). EEG alpha and theta oscillations reflect cognitive and memory performance: a review and analysis. Brain Res. Brain Res. Rev. *29*, 169–195.

Klimesch, W., Freunberger, R., Sauseng, P., and Gruber, W. (2008). A short review of slow phase synchronization and memory: evidence for control processes in different memory systems? Brain Res. *1235*, 31–44.

Kopell, N.J., Gritton, H.J., Whittington, M.A., and Kramer, M.A. (2014). Beyond the connectome: the dynome. Neuron *83*, 1319–1328.

Kucewicz, M.T., Berry, B.M., Miller, L.R., Khadjevand, F., Ezzyat, Y., Stein, J.M., Kremen, V., Brinkmann, B.H., Wanda, P., Sperling, M.R., et al. (2018). Evidence for verbal memory enhancement with electrical brain stimulation in the lateral temporal cortex. Brain *141*, 971–978.

Kuznetsova, A., Brockhoff, P.B., and Christensen, R.H.B. (2017). lmerTest Package: Tests in Linear Mixed Effects Models. J. Stat. Softw. *82*, 1–26.

Lancaster, J.L., Woldorff, M.G., Parsons, L.M., Liotti, M., Freitas, C.S., Rainey, L., Kochunov, P.V., Nickerson, D., Mikiten, S.A., and Fox, P.T. (2000). Automated Talairach atlas labels for functional brain mapping. Hum. Brain Mapp. *10*, 120–131.

Lee, J., and Park, S. (2005). Working memory impairments in schizophrenia: a meta-analysis. J. Abnorm. Psychol. *114*, 599–611.

Lee, T.W., Girolami, M., Bell, A.J., and Sejnowski, T.J. (2000). A unifying information-theoretic framework for independent component analysis. Comput. Math. Appl. *39*, 1–21.

Lempka, S.F., and McIntyre, C.C. (2013). Theoretical analysis of the local field potential in deep brain stimulation applications. PLoS One *8*, e59839.

Lobier, M., Palva, J.M., and Palva, S. (2018). High-alpha band synchronization across frontal, parietal and visual cortex mediates behavioral and neuronal effects of visuospatial attention. Neuroimage *165*, 222–237.

Luber, B., Kinnunen, L.H., Rakitin, B.C., Ellsasser, R., Stern, Y., and Lisanby, S.H. (2007). Facilitation of performance in a working memory task with rTMS stimulation of the precuneus: frequency- and time-dependent effects. Brain Res. *1128*, 120–129.

Lund, U., and Agostinelli, C. (2017). R package 'circular': Circular Statistics (version 0.4-93). https://r-forge.r-project.org/projects/circular/.

Ma, L., Steinberg, J.L., Hasan, K.M., Narayana, P.A., Kramer, L.A., and Moeller, F.G. (2012). Working memory load modulation of parieto-frontal

connections: evidence from dynamic causal modeling. Hum. Brain Mapp. *33*, 1850–1867.

Meltzer, J.A., Zaveri, H.P., Goncharova, I.I., Distasio, M.M., Papademetris, X., Spencer, S.S., Spencer, D.D., and Constable, R.T. (2008). Effects of working memory load on oscillatory power in human intracranial EEG. Cereb. Cortex *18*, 1843–1855.

Mottaghy, F.M. (2006). Interfering with working memory in humans. Neuroscience *139*, 85–90.

Nee, D.E., Brown, J.W., Askren, M.K., Berman, M.G., Demiralp, E., Krawitz, A., and Jonides, J. (2013). A meta-analysis of executive components of working memory. Cereb. Cortex *23*, 264–282.

Nolte, G., Bai, O., Wheaton, L., Mari, Z., Vorbach, S., and Hallett, M. (2004). Identifying true brain interaction from EEG data using the imaginary part of coherency. Clin. Neurophysiol. *115*, 2292–2307.

Ojemann, G.A., Ojemann, J., and Ramsey, N.F. (2013). Relation between functional magnetic resonance imaging (fMRI) and single neuron, local field potential (LFP) and electrocorticography (ECoG) activity in human cortex. Front. Hum. Neurosci. *7*, 34.

Oostenveld, R., Fries, P., Maris, E., and Schoffelen, J.M. (2011). FieldTrip: open source software for advanced analysis of MEG, EEG, and invasive electrophysiological data. Comput. Intell. Neurosci. *2011*, 156869.

Osaka, N., Otsuka, Y., Hirose, N., Ikeda, T., Mima, T., Fukuyama, H., and Osaka, M. (2007). Transcranial magnetic stimulation (TMS) applied to left dorsolateral prefrontal cortex disrupts verbal working memory performance in humans. Neurosci. Lett. *418*, 232–235.

Owen, A.M., McMillan, K.M., Laird, A.R., and Bullmore, E. (2005). N-back working memory paradigm: a meta-analysis of normative functional neuroimaging studies. Hum. Brain Mapp. *25*, 46–59.

Palva, J.M., Monto, S., Kulashekhar, S., and Palva, S. (2010). Neuronal synchrony reveals working memory networks and predicts individual memory capacity. Proc. Natl. Acad. Sci. USA *107*, 7580–7585.

Payne, L., and Kounios, J. (2009). Coherent oscillatory networks supporting short-term memory retention. Brain Res. *1247*, 126–132.

Penny, W.D., Friston, K.J., Ashburner, J.T., Kiebel, S.J., and Nichols, T.E. (2011). Statistical Parametric Mapping: The Analysis of Functional Brain Images (Academic Press).

Polanía, R., Nitsche, M.A., Korman, C., Batsikadze, G., and Paulus, W. (2012). The importance of timing in segregated theta phase-coupling for cognitive performance. Curr. Biol. *22*, 1314–1318.

Postle, B.R., Ferrarelli, F., Hamidi, M., Feredoes, E., Massimini, M., Peterson, M., Alexander, A., and Tononi, G. (2006). Repetitive transcranial magnetic stimulation dissociates working memory manipulation from retention functions in the prefrontal, but not posterior parietal, cortex. J. Cogn. Neurosci. *18*, 1712–1722.

Quentin, R., Elkin Frankston, S., Vernet, M., Toba, M.N., Bartolomeo, P., Chanes, L., and Valero-Cabré, A. (2016). Visual Contrast Sensitivity Improvement by Right Frontal High-Beta Activity Is Mediated by Contrast Gain Mechanisms and Influenced by Fronto-Parietal White Matter Microstructure. Cereb. Cortex *26*, 2381–2390.

Raghavachari, S., Kahana, M.J., Rizzuto, D.S., Caplan, J.B., Kirschen, M.P., Bourgeois, B., Madsen, J.R., and Lisman, J.E. (2001). Gating of human theta oscillations by a working memory task. J. Neurosci. *21*, 3175–3183.

Riddle, J., Hwang, K., Cellier, D., Dhanani, S., and D'Esposito, M. (2019). Causal Evidence for the Role of Neuronal Oscillations in Top-Down and Bottom-Up Attention. J. Cogn. Neurosci. *31*, 768–779.

Rottschy, C., Langner, R., Dogan, I., Reetz, K., Laird, A.R., Schulz, J.B., Fox, P.T., and Eickhoff, S.B. (2012). Modelling neural correlates of working memory: a coordinate-based meta-analysis. Neuroimage *60*, 830–846.

Roux, F., and Uhlhaas, P.J. (2014). Working memory and neural oscillations: $\alpha$-$\gamma$ versus $\theta$-$\gamma$ codes for distinct WM information? Trends Cogn. Sci. *18*, 16–25.

Sarnthein, J., Petsche, H., Rappelsberger, P., Shaw, G.L., and von Stein, A. (1998). Synchronization between prefrontal and posterior association cortex during human working memory. Proc. Natl. Acad. Sci. USA *95*, 7092–7096.

Sauseng, P., Klimesch, W., Doppelmayr, M., Pecherstorfer, T., Freunberger, R., and Hanslmayr, S. (2005a). EEG alpha synchronization and functional coupling during top-down processing in a working memory task. Hum. Brain Mapp. *26*, 148–155.

Sauseng, P., Klimesch, W., Schabus, M., and Doppelmayr, M. (2005b). Fronto-parietal EEG coherence in theta and upper alpha reflect central executive functions of working memory. Int. J. Psychophysiol. *57*, 97–103.

Sauseng, P., Klimesch, W., Heise, K.F., Gruber, W.R., Holz, E., Karim, A.A., Glennon, M., Gerloff, C., Birbaumer, N., and Hummel, F.C. (2009). Brain oscillatory substrates of visual short-term memory capacity. Curr. Biol. *19*, 1846–1852.

Sauseng, P., Griesmayr, B., Freunberger, R., and Klimesch, W. (2010). Control mechanisms in working memory: a possible function of EEG theta oscillations. Neurosci. Biobehav. Rev. *34*, 1015–1022.

Schack, B., Klimesch, W., and Sauseng, P. (2005). Phase synchronization between theta and upper alpha oscillations in a working memory task. Int. J. Psychophysiol. *57*, 105–114.

Shine, J.M., Bissett, P.G., Bell, P.T., Koyejo, O., Balsters, J.H., Gorgolewski, K.J., Moodie, C.A., and Poldrack, R.A. (2016). The dynamics of functional brain networks: integrated network states during cognitive task performance. Neuron *92*, 544–554.

Siegle, J.H., and Wilson, M.A. (2014). Enhancement of encoding and retrieval functions through theta phase-specific manipulation of hippocampus. eLife *3*, e03061.

Stam, C.J., Nolte, G., and Daffertshofer, A. (2007). Phase lag index: assessment of functional connectivity from multi channel EEG and MEG with diminished bias from common sources. Hum. Brain Mapp. *28*, 1178–1193.

Suthana, N., Haneef, Z., Stern, J., Mukamel, R., Behnke, E., Knowlton, B., and Fried, I. (2012). Memory enhancement and deep-brain stimulation of the entorhinal area. N. Engl. J. Med. *366*, 502–510.

Thut, G., Schyns, P.G., and Gross, J. (2011). Entrainment of perceptually relevant brain oscillations by non-invasive rhythmic stimulation of the human brain. Front. Psychol. *2*, 170.

Vinck, M., Oostenveld, R., van Wingerden, M., Battaglia, F., and Pennartz, C.M. (2011). An improved index of phase-synchronization for electrophysiological data in the presence of volume-conduction, noise and sample-size bias. Neuroimage *55*, 1548–1565.

Violante, I.R., Li, L.M., Carmichael, D.W., Lorenz, R., Leech, R., Hampshire, A., Rothwell, J.C., and Sharp, D.J. (2017). Externally induced frontoparietal synchronization modulates network dynamics and enhances working memory performance. eLife *6*, e22001.

Wager, T.D., and Smith, E.E. (2003). Neuroimaging studies of working memory: a meta-analysis. Cogn. Affect. Behav. Neurosci. *3*, 255–274.

Winawer, J., and Parvizi, J. (2016). Linking Electrical Stimulation of Human Primary Visual Cortex, Size of Affected Cortical Area, Neuronal Responses, and Subjective Experience. Neuron *92*, 1213–1219.

Yarkoni, T., Poldrack, R.A., Nichols, T.E., Van Essen, D.C., and Wager, T.D. (2011). Large-scale automated synthesis of human functional neuroimaging data. Nat. Methods *8*, 665–670.

Zalesky, A., Fornito, A., and Bullmore, E.T. (2010). Network-based statistic: identifying differences in brain networks. Neuroimage *53*, 1197–1207.

Zanos, S., Rembado, I., Chen, D., and Fetz, E.E. (2018). Phase-Locked Stimulation during Cortical Beta Oscillations Produces Bidirectional Synaptic Plasticity in Awake Monkeys. Curr. Biol. *28*, 2515–2526.e4.

Zanto, T.P., Rubens, M.T., Thangavel, A., and Gazzaley, A. (2011). Causal role of the prefrontal cortex in top-down modulation of visual processing and working memory. Nat. Neurosci. *14*, 656–661.

Zoefel, B., Archer-Boyd, A., and Davis, M.H. (2018). Phase Entrainment of Brain Oscillations Causally Modulates Neural Responses to Intelligible Speech. Curr. Biol. *28*, 401–408.e55.

# STAR★METHODS

## KEY RESOURCES TABLE

| REAGENT or RESOURCE | SOURCE | IDENTIFIER |
|---|---|---|
| Deposited Data | | |
| Task Performance | This paper | https://osf.io/vx5jb/ |
| iEEG Data | This paper | https://osf.io/vx5jb |
| Software and Algorithms | | |
| Psychtoolbox | Brainard, 1997 | http://psychtoolbox.org/download; RRID: SCR_002881 |
| MATLAB R2018b | Mathworks, Inc | https://www.mathworks.com/; RRID: SCR_001622 |
| EEGLAB 14.0.0.b | Delorme and Makeig, 2004 | https://github.com/sccn/eeglab; RRID: SCR_007292 |
| Fieldtrip | Oostenveld et al., 2011 | https://github.com/fieldtrip/fieldtrip; RRID: SCR_004849 |
| 3D Slicer | Fedorov et al., 2012 | https://www.slicer.org; RRID: SCR_005619 |
| Talairach Client | Lancaster et al., 2000 | http://www.talairach.org/client.html; RRID: SCR_000448 |
| Neurosynth | Yarkoni et al., 2011 | https://neurosynth.org; RRID: SCR_006798 |
| SPM12 | Penny et al., 2011 | https://www.fil.ion.ucl.ac.uk/spm/software/spm12/; RRID: SCR_007037 |
| MarsBaR | Brett et al., 2002 | http://marsbar.sourceforge.net; RRID: SCR_009605 |
| Lmertest | Kuznetsova et al., 2017 | https://cran.r-project.org/web/packages/lmerTest/index.html; RRID: SCR_015656 |
| Circular | Lund and Agostinelli, 2017 | https://cran.r-project.org/web/packages/circular/ |

## LEAD CONTACT AND MATERIALS AVAILABILITY

Further information and requests for resources should be directed to and will be fulfilled by the Lead Contact, Flavio Frohlich (flavio_frohlich@med.unc.edu). This study did not generate new unique reagents.

## EXPERIMENTAL MODEL AND SUBJECT DETAILS

### Participants

All experimental procedures were approved by the Institutional Review Board of University of North Carolina at Chapel Hill and informed consent was obtained from participants. Participants (n = 3) were recruited by invitation from patients who underwent invasive monitoring for epilepsy surgery planning. The participant clinical details are provided in 'Clinical Information' table. The location of electrodes in all participants were completely dictated by the clinical needs of the individual participant. The electrodes covered bilateral frontal, parietal, and temporal cortices (Figure S1).

#### *Clinical Information*

| Participant ID | Sex | Age | Seizure Onset Zones |
|---|---|---|---|
| P1 | F | 20 | Bilateral hippocampus and temporal lobes |
| P2 | M | 24 | Bilateral hippocampus, amygdala, postcentral gyrus |
| P3 | F | 46 | Bilateral posterior frontal cortex |

## METHOD DETAILS

### Working Memory Task

Participants performed a Sternberg working memory task that has been previously used in ECoG studies (Alagapan et al., 2019a; Meltzer et al., 2008; Raghavachari et al., 2001). The Sternberg task allows a separation of different cognitive processes involved in working memory into different epochs: encoding, maintenance, and retrieval (Figure 1B). Each trial began with a fixation cross presented for 1000 ms. In the encoding epoch, participants were presented with a sequence of letters from the English alphabet one letter at a time. Each letter was presented for 500 ms. Following the encoding epoch, a blank screen was presented for 2000 ms which served as the maintenance epoch. Next, a single letter (probe) was presented on the screen for 3000 ms. The participants were instructed to indicate if the probe was present in the encoding epoch or not using custom joysticks that interfaced with the

task administration laptop through a USB response box (Black Box Toolkit, Sheffield, UK). P3 was not able to use the joysticks due to history of stroke affecting motor function in their right hand and responded using the keyboard of the laptop with their left hand only. The task was programmed in MATLAB using Psychtoolbox (Brainard, 1997).

Participants completed the task in two sessions – a baseline session and a stimulation session. In the baseline session, the task consisted of memory arrays of two different lengths (WM load). In the stimulation session, the WM load was fixed to maximize the number of trials in each stimulation condition. The experimental parameters used for the participants are listed in the 'Experimental Parameters' table.

Before the baseline session, participants performed practice trials (between 10 and 20 trials) to familiarize themselves with the task. We calculated accuracy during the practice trials in order to determine the list length for the experiment. Any list length of which the participant was able to perform at greater than 60% accuracy was set as the list length for the participant's baseline session. The data from this practice session was not systematically analyzed.

***Experimental Parameters***

| Participant ID | Baseline WM Load | Baseline No. Trials/Load | Stimulation WM Load | Stimulation No. Trials/Condition | Stimulation Electrode Location | Stimulation Frequency |
|---|---|---|---|---|---|---|
| P1 | 3,5 | 30 | 5 | 30 | Left anterior superior frontal gyrus, Left inferior precentral sulcus | 4 Hz |
| P2 | 5,7 | 40 | 7 | 30 in-phase, 36 anti-phase, 34 Sham | Left inferior frontal junction, left superior parietal lobule | 10 Hz |
| P3 | 5,7 | 40 | 5 | 40 | Right anterior middle frontal gyrus, right superior intraparietal sulcus | 10 Hz |

### ECoG Data Acquisition and Direct Cortical Stimulation

ECoG data were recorded using a 128-channel EEG system (NetAmps 410, Electrical Geodesics Inc, Eugene, Oregon, United States) at 1000 Hz sampling rate. Stimulation was delivered using Cerestim M96 cortical stimulator (Blackrock Microsystems, Salt Lake City, Utah, United States). Stimulation consisted of a train of biphasic pulses 2 mA in amplitude, 200 μs in duration per phase of the biphasic pulse with a 55 μs interval between the positive going and negative going phase. The inter-pulse-interval was adjusted according to the stimulation frequency. Stimulation was applied between two pairs of electrodes identified from functional connectivity analysis as described in the next subsection. The timing of pulses between the two pairs was in-phase, i.e., stimulation was applied simultaneously between the two electrode pairs (Figure 1C). We hypothesized that in-phase stimulation would improve WM performance. The active control was anti-phase stimulation, i.e., stimulation between the first pair and second pair was offset by half the inter-pulse-interval (Figure 1C). Both in-phase and anti-phase stimulation was time-locked to the start of the encoding epoch and lasted the entire epoch. Stimulation was triggered using MATLAB wrapper functions provided by the manufacturer of the cortical stimulator. In addition, a control condition where no stimulation was applied (sham) was also included to control for the general effect of stimulation on performance. The three stimulation conditions (in-phase, anti-phase, and sham) were randomly interleaved for each task block.

The stimulation intensity used in the study was set at 2 mA, which is less than the intensities at which sensory and motor effects are observed clinically. In addition to this, 2 of the 3 participants (P2 and P3) filled out a questionnaire assessing stimulation side-effects after the stimulation experiment. Neither patients were able to attribute any side-effects to stimulation.

### Removal of Electrical Stimulation Artifacts

Electrical stimulation artifacts were removed using an independent component analysis (ICA) based approach as demonstrated in our previous work (Alagapan et al., 2019a). Artifacts appear as stereotypical waveforms in iEEG signals. Blind signal separation using ICA separates the iEEG signal into components that contain only artifact waveforms and other components that contain the rest of the signal. The components containing artifacts were then rejected and the remaining components were used to reconstruct the artifact free signal. We used the infomax algorithm (Lee et al., 2000) available as a part of EEGLab toolbox for computing independent components. Following artifact suppression, the signals were re-referenced to the average of all signals. Refer to Figure S3 for example traces before and after removal of artifacts.

### Identification of Electrode Locations

The anatomical locations of the electrodes were identified using steps described previously (Alagapan et al., 2019a; Alagapan et al., 2016).The electrode locations were extracted from postoperative CT images using 3D Slicer (Fedorov et al., 2012). Electrode locations were manually marked in the postoperative CT image. The postoperative CT was coregistered to preoperative MRI in Slicer following which the preoperative MRI was coregistered with MNI atlas (Fonov et al., 2011), thereby transferring the electrode locations to the MNI space.

### Determining Meta-Analysis-Based WM Network

We used a meta-analysis-based approach to identify regions activated by a variety of WM tasks. Using Neurosynth, we acquired the association test map for 'Working Memory' that was derived from 1091 studies. Neurosynth is an automated tool that synthesizes activation coordinates (in MNI or Talairach space) published in neuroimaging articles along with the associated keywords to generate probabilistic mappings between the keywords and neuroimaging substrates. The probabilistic maps are available for download from the website neurosynth.org. The association test map consisted of z-scores, corrected with false discovery rate (FDR) at an alpha value of 0.01, from a two-way ANOVA testing for the presence of a non-zero association between the term 'working Memory' and voxel activation (Yarkoni et al., 2011). The association map provides a measure of selective activation, i.e., the activation in a region occurring more consistently in studies with the keyword than studies that do not. We defined 8 mm regions of interest (ROIs) around each electrode in the Montreal Neurological Institute (MNI) space using custom written scripts and the MarsBaR toolbox in SPM12 (Brett et al., 2002; Penny et al., 2011). Next, we determined the z-scores from the association map within these ROIs (electrodes) and computed the mean z-score for each electrode. Any electrode that had a mean z-score greater than 0 was defined to be part within the mWM network and was included in analysis. Using this approach, the number of electrodes in WM regions differed for each participant. In participant P1, 21 out of 80 electrodes were in WM regions, in participant P2, 23 out of 89 electrodes were in WM regions and in participant P3, 34 out of 105 electrodes were in WM regions.

## QUANTIFICATION AND STATISTICAL ANALYSIS

### Data Analysis

All data analysis was performed using custom written MATLAB scripts utilizing functions from the EEGLAB (Delorme and Makeig, 2004) and Fieldtrip toolboxes (Oostenveld et al., 2011). Electrodes over seizure focus were excluded from analysis.

### Selection of Stimulation Electrodes

ECoG data collected during the baseline session was used to determine functionally connected electrodes. The continuous data were band-pass filtered between 1 and 50 Hz using an FIR filter and re-referenced to the average of all intracranial electrodes using functions from EEGLAB toolbox. The data were then segmented into trials containing the different epochs. Functional connectivity was determined using debiased weighted phase lag index square (dWPLI) implemented in Fieldtrip toolbox. The measure is a composite of phase lag index, which captures consistency in phase lag between two time oscillatory signals (Stam et al., 2007), and the imaginary part of coherence which ignores zero phase lag interactions (Nolte et al., 2004). DWPLI has been shown to provide a better estimate of phase-synchronization in the presence of volume conduction and the debiased estimate has higher statistical power (Vinck et al., 2011). DWPLI was computed for the fixation, encoding, and retention epochs separately. The dWPLI spectrum was visually inspected to identify peak frequency. Then the dWPLI spectrum was averaged in a frequency band (peak frequency $\pm$ 1.5 Hz) to get an adjacency matrix. The stimulation electrodes were chosen based on the connections that had high dWPLI values. While we did not verify statistical significance of the connections before the stimulation experiment, post hoc analysis of baseline data using a nonparametric approach revealed the electrodes chosen for stimulation in P1 and P2 were statistically significant. A trial-shuffle method was used for correcting for false-positives post hoc. The data corresponding to channels were shuffled 1000 times across trials (with the same cognitive load) to destroy temporal relationships and dWPLI adjacency matrices were computed for each shuffle. Any connection whose dWPLI value was greater than the $95^{th}$ percentile of corresponding shuffled estimates was deemed statistically significant. Standard deviation of dWPLI spectra was estimated using a jackknife approach as follows. Trials were left out one at a time and dWPLI spectrum was estimated using this reduced dataset. The variance of these estimates was deemed to be the standard deviation of the dWPLI spectrum. The strength of functional connectivity was strongest between neighboring electrodes followed by electrodes within the same anatomical region, i.e., frontal cortex or parietal cortex. Since we were interested in modulating long-range functional connectivity, we ignored electrode pairs that were neighbors. In addition, connections that were present in the fixation epoch and between electrodes over seizure foci were ignored as the former may reflect preparatory attentional components of network activity and the latter may reflect pathological connectivity.

### Estimation of Functional Connectivity

DWPLI was computed for the stimulation session (epoched by stimulation condition) in the same manner as the baseline session (epoched by WM load) using functions from EEGlab and Fieldtrip toolboxes. In addition, coherence was also computed for the stimulation session. Adjacency matrices were derived from a 3 Hz band centered on the frequency of interest. Phase lag was derived from the mean cross-spectrum across trials in a 2 Hz band centered on the frequency of stimulation. For pairwise comparisons between stimulation conditions, the difference in adjacency matrices were computed. Only connections that passed statistical significance threshold were included for further analysis. Statistical significance was computed using a permutation-based approach. Trial labels were shuffled, and adjacency matrices were computed for each condition. This procedure was repeated for 1000 iterations. Pairwise differences were computed for each iteration to generate a null distribution. Any pairwise difference in the non-shuffled adjacency matrices that were greater (or lesser) than 95% of the null distribution differences was deemed statistically significant. To account for the false positives that may arise from multiple comparisons in the adjacency matrices, false discovery rate (FDR) correction (Genovese et al., 2002) was performed with a threshold of 0.1. FDR was initially developed by Benjamini and Hochberg (1995)

and has been commonly used to account for multiple comparisons in many fields including analysis of brain networks (Bassett et al., 2011; Shine et al., 2016; Accolla et al., 2016) as well as neuroimaging in general (Bennett et al., 2009). FDR sets a limit on the *false positives relative to true positives* while shuffle correction (alpha) sets a limit on the *false positives relative to true negatives*. In practice, this means a much stricter threshold for p values that depends on the distribution of p values. FDR has been shown to be conservative when the number of comparisons is large, as in the case when connections within networks are considered (Zalesky et al., 2010). Therefore, we chose to use an FDR correction of 0.1 (instead of 0.05) to allow for enough connections in the network to accurately capture the general pattern of functional connectivity within the working memory network. Applying the FDR correction for each network separately, the p value threshold for determining significance were lesser than 0.05 (ranged from $< 0.001$ to 0.022).

Network sparsity was determined from the edge density in the network i.e., percentage of possible connections that were actually present after the false discovery rate correction to eliminate connections that might have been due to random chance.

### Statistical Analysis

All statistical analyses were performed using custom-written scripts in R and MATLAB. We used linear mixed models with reaction times as the dependent variable and stimulation condition as fixed factor (with three levels) and participants as random factor to test the association between reaction time and stimulation condition accounting for the variability that may be introduced by random differences in participants. We used chi-square test of independence to test for the presence of association between stimulation condition and accuracy. To test the effect of stimulation condition on functional connectivity changes, we used linear mixed models to account for variability between participants. We fit models with intercepts and participants as random factors to test non-zero differences between conditions. We used Watson-Wheeler test, a non-parametric test designed specifically for circular data, to test differences in phase lags between comparisons. Phase lags were pooled across participants as the as there were not sufficient samples to infer at a participant level. Linear mixed models were fitted using *'lmertest'* package (Kuznetsova et al., 2017). The package uses a Sattherwaite approximation for degrees of freedom for ANOVA. Circular statistics were computed using *'circular'* package (Lund and Agostinelli, 2017).

## DATA AND CODE AVAILABILITY

Code for analysis and the raw data are available at https://osf.io/vx5jb/